

**The Role of Hydrogen in the Growth of Carbon Nanotubes:
A Study of the Catalyst State and Morphology**

by

Jin Suk Calvin Kim

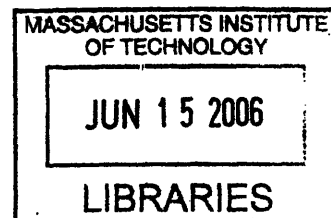
Submitted to the Department of Materials Science and Engineering in partial fulfillment
of the Requirements for the
Degree of

BACHELOR OF SCIENCE

at the

MASSACHUSETTS INSTITUTE OF TECHNOLOGY

[June 2006]
May 2006



ARCHIVES

© 2006 JIN SUK CALVIN KIM
All rights reserved

The author hereby grants to MIT permission to reproduce and to distribute publicly paper
and electronic copies of this thesis document in whole or in part.

Signature of Author _____
Department of Materials Science and Engineering
May 22nd, 2006

Certified by _____
Carl V. Thompson
Stavros Salapatas Professor
Thesis Supervisor, Department of Materials Science and Engineering

Accepted by _____
Professor Caroline Ross
Chair of the Undergraduate Program
Department of Materials Science and Engineering

The Role of Hydrogen in the Growth of Carbon Nanotubes: A Study of the Catalyst State and Morphology

By

Jin Suk Calvin Kim

Submitted to the Department of Materials Science and Engineering on
May 22nd, 2006, in partial fulfillment of the
requirements for the degree of
Bachelor of Science in Materials Science and Engineering

Abstract

The role of hydrogen in chemical vapor decomposition (CVD) of C_2H_4 for growth of carbon nanotubes (CNTs) was investigated. Fe/Al_2O_3 (1/10 nm) catalyst layers were used for growth on Si substrates and the times at which H_2 was introduced during the 40 minute temperature ramp, 15 minute annealing (without C_2H_4), and 15 minute growth (during which C_2H_4 was flowing) stages was varied. When H_2 was introduced before heating, CNTs grew to a length of ~ 0.3 mm. However, CNT growth was severely suppressed when H_2 was introduced at different points during temperature ramp. Recovery of CNT growth was observed when H_2 was introduced during the annealing and growth stages. Under optimum conditions, a ~ 1 mm-thick carpet of CNTs could be obtained. The chemical state and morphology of the catalysts as a function of the time of H_2 introduction were examined using XPS and AFM, respectively. We found that the as-deposited state of Fe was an iron oxide, due to reaction with O_2 in the atmosphere, and that the H_2 reduced the iron oxide to different oxidation states, depending on the time of H_2 introduction. AFM inspection showed that surface roughness could also be correlated with areas of vertical CNT growth. A preliminary model for CNT growth in which the oxidation state of iron determines its catalytic activity is proposed, and it is argued that the effects of H_2 seen in this study are the result of the interplay of H_2 reduction and oxidation associated with a low partial of O_2 in CVD gases.

Thesis Supervisor: Carl V. Thompson

Title: Stavros Salapatas Professor, Department of Materials Science and Engineering

Table of Contents

	Page #
ABSTRACT	2
TABLE OF CONTENTS	3
LIST OF FIGURES	4
LIST OF TABLES	5
ACKNOWLEDGEMENTS	6
Chapter 1: Introduction	7
Chapter 2: Background Theory	8
2.1 Carbon Nanotube: Characterization	8
2.2 Growth Systems	10
2.3 Hydrogen's Role in Pretreatment and During Growth	12
2.4 Chemical State of the Fe Catalyst	14
2.5 Chemical Morphology: Size	16
Chapter 3: Experimental Procedure	18
3.1 E-beam Evaporation	18
3.2 CVD Furnace Arrangement	18
3.3 CNT Growth Conditions	20
3.4 CNT Analysis by SEM and Catalyst Morphology Analysis by AFM	21
3.5 Catalyst Chemical State Analysis by XPS	22
Chapter 4: Results	24
4.1 SEM Elucidates the Effect of H ₂	24
4.2 Catalyst Morphology by AFM	33
4.3 Chemical State of the Catalyst by XPS	38
Chapter 5: Discussion	44
5.1 CNT Growth Examined by SEM	44
5.2 Catalyst Morphology	45
5.3 Catalyst Chemical State	46
5.4 Proposed Model	47
Chapter 6: Conclusions	49
Chapter 7: Future Research	50
BIBLIOGRAPHY	51

List of Figures

<u>Figure</u>	<u>Title</u>	<u>Page #</u>
1	Carbon Nanotube Formation	8
2	Three Different Types of Carbon Nanotubes	9
3	Assembly Methods	12
4	Experimental Setup of CNT Furnace Chamber	19
5	Experimental Design of Hydrogen Introduction	21
6	SEM Images of CNTs Resulting from Controls	25
7	SEM of CNTs of H ₂ Introduction during Temp. Ramp	26
8	SEM Images of H ₂ Introduction during Annealing	28
9	SEM of CNTs H ₂ Introduction during Growth	29
10	SEM of CNTs Exposed to 1 min and 30 sec of H ₂	30
11	Experimental Conditions and CNT Growth Results	32
12	AFM of Fe / Al ₂ O ₃	34
13	Summary AFM of Fe / Al ₂ O ₃	35
14	AFM of Fe / Al ₂ O ₃ at +5 minutes and 600°C	37
15	XPS of Fe / Al ₂ O ₃	40
16	XPS of Fe / Al ₂ O ₃ before and after growth	42

List of Tables

<u>Table</u>	<u>Title</u>	<u>Page #</u>
1	Summary of CNT Heights	32

Acknowledgements

The author would like to especially thank Professor Carl V. Thompson for his discussions and his general guidance throughout the research process. Many thanks to Gilbert Nessim and Jihun Oh for their invaluable assistance and teachings and especially to Jihun Oh for his background knowledge. They contributed much in the comprehension of the observed results.

The author would further like to express gratitude to Anastatios John Hart and Donatello Acquaviva for their help in further discussions and experimentations.

Chapter 1

Introduction

Carbon nanotubes (CNTs) are graphene sheets rolled into tubes ranging from 0.8 nm to 200 nm in diameter. Since their discovery in 1991 by Iijima, carbon nanotubes have generated a large amount of interest [16]. They have been identified as ideal components for use in biosensors, field emission displays, nanoelectronics, and hydrogen storage devices. CNTs' unique properties account for this applicability: CNTs have high electronic conductivity, thermal conductivity, and great mechanical strength along their axis, which depend on their diameter, length, chirality, and twist. However, currently major obstacles are present in the application of carbon nanotubes. Specifically, the exact growth mechanism of CNTs and their resulting properties are not yet well understood. Hence, there has been an ongoing effort to understand the growth of CNTs. Our work especially focuses on CNTs directly grown from a catalyst on a substrate using a method called thermal chemical vapor deposition (CVD). This method was utilized in our study because CNTs directly attached to a substrate presents an additional advantage for applicational use since these CNTs do not require additional adhering steps to a substrate. Here we examine the chemical state and morphology of the catalyst, which induces growth of CNTs, to propose a model for the growth of CNTs from a metal catalyst.

Chapter 2

Background Theory

2.1 Carbon Nanotube: Characterization

The defining characteristic of a carbon nanotube is its structure. A carbon nanotube is crystalline graphite, which forms a cylindrical structure based on a hexagonal lattice of carbon atoms. A two dimensional structure of a carbon nanotube is shown in Figure 1. The properties of a carbon nanotube depend on its chiral angle and diameter. Based on chirality, there are three types of carbon nanotubes: zigzag, armchair, and chiral (Figure 2). These three types are described by their (n, m) values. Armchair nanotubes are formed when $n = m$ with a resulting chiral angle of 30° , and zigzag carbon nanotubes are formed when either n or m is zero with a resulting chiral angle of 0° . All other nanotubes are known as chiral nanotubes and have chiral angles between 0° and 30° . The chiral angle can be calculated by Equation (1).

$$(1) \quad \text{Chiral Angle} = \tan^{-1}(\sqrt{3}n/(2m + n))$$

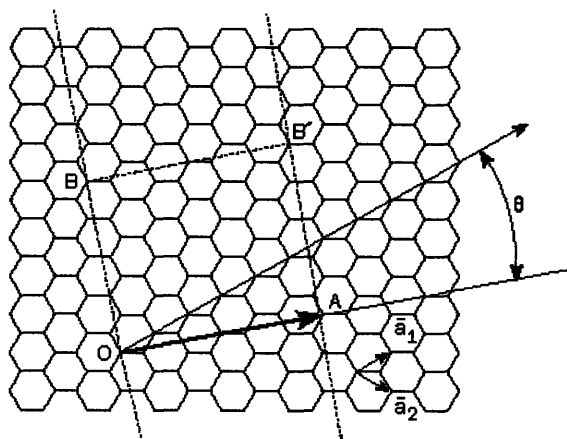


Figure 1. Carbon nanotube formation. Two Dimensional [15]

The chiral vector, $C_h = n\hat{a}_1 + m\hat{a}_2$, is shown on this hexagonal lattice where \hat{a}_1 and \hat{a}_2 are unit vectors, and n and m are integers. The chiral angle, q , is measured relative to the direction defined by \hat{a}_1 . To form the nanotube, this cell is rolled up so that O meets A and B meets B', and the two ends are capped with half of a fullerene molecule [15].

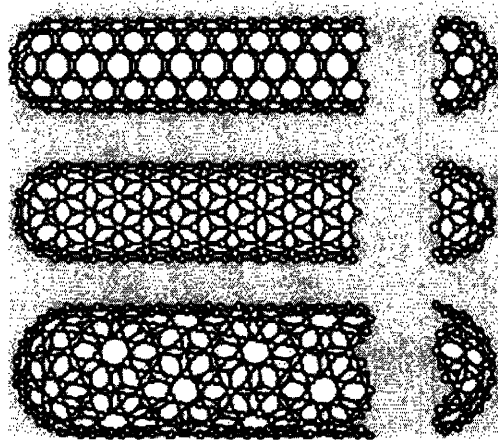


Figure 2. Three different types of carbon nanotubes [15].

A (5, 5) armchair nanotube, a (9, 0) zigzag nanotube, and a (10, 5) chiral nanotube are shown from top to bottom, respectively. The n and m values determine the diameter of the tube [15].

Chirality also determines electrical conductivity. A metallic (n, m) carbon nanotube forms when $n - m = 3q$, where q is an integer. Therefore, all armchair nanotubes are metallic, and a third of zigzag nanotubes are metallic. The other remaining CNT types are semi-metallic. In theory, a CNT can carry an electron current a thousand times greater than silver or copper.

Another important characteristic of a carbon nanotube is its diameter. The diameter is one fourth of the length of its chiral vector, and can be found by Equation (2),

$$(2) \quad d_t = (\sqrt{3}/p)a_{c-c}(m^2 + mn + n^2)^{1/2}$$

where a_{c-c} is the distance between neighboring carbon atoms in a flat sheet. As a result, two types of carbon nanotubes may form: single walled carbon nanotubes (SWNTs) and multi-walled nanotubes (MWNTs).

MWNTs are composed of multiple layers of graphene sheets rolled in on themselves. Two model of structure have been proposed for MWNTs: the Russian Doll and the Parchment. In the Russian Doll model, multiple graphene sheets are rolled in concentric cylinders; in the Parchment model, a single graphene sheet is rolled in on

itself. The other kind of CNT is a SWNT, which consists of one cylinder and has a diameter of around 1 nm. They exhibit important electronic properties, which the MWNTs do not possess. As a result, SWNTs are the most attractive candidates for microscale and nanoscale electronics.

Other properties of carbon nanotubes include thermal conductivity and high tensile strength and elasticity. Carbon nanotubes have very good thermal conductivity along its axis known as “ballistic conduction.” Ballistic conduction allows electrons to move through materials without collisions. Finally, the *sp*² covalent bonds of carbon nanotubes render it one of the strongest materials known today. The tensile strength of carbon nanotubes has been reported to be greater than 63 GPa, and the elastic modulus on the order of 1 TPa.

2.2 Growth Systems

A number of methods have been developed to grow carbon nanotubes including laser ablation, arc discharge, thermal chemical vapor deposition (CVD), and plasma enhanced chemical vapor deposition (PECVD). Arc discharge, one of the easiest methods for CNT production, utilizes arc vaporization of carbon rods at the two ends. An alternative process, laser ablation, also involves laser vaporization. The advantages of these two systems are that they are fairly simple. In addition, the arc discharge method can produce CNTs in bulk quantity. For nanoelectronic applications, however, the arc discharge and laser ablation methods are not efficient for CNT growth; for devices such as field emission and other templated electronics, controlled growth is needed, which is much easier in CVD. CVD also provides high throughput, allows for direct growth on a desired substrate unlike the first two methods, and results in uniform growth. Thus,

chemical vapor deposition is the preferred method and has been used mainly to grow a variety of structures which can be patterned and manipulated frequently in design.

There are two types of chemical vapor deposition techniques, PECVD and thermal CVD. PECVD uses a high temperature substrate and plasma, which is called glow discharge, to facilitate decomposition of the precursors to enable growth of CNTs at lower temperatures. Thermal CVD systems utilize only heat to decompose the precursors so that higher temperatures are required than in PECVD. For the heat source, there are two main options: a cold-wall CVD system, which has a cold wall and hot substrate, or a hot-wall CVD. Also, in a thermal CVD system, catalysts, commonly metals such as Co, Ni, or Fe, are deposited via thermal or e-beam evaporation or via spinning of a liquid solution of particles, onto a substrate. Gases are then flown through a heated tube at 700 – 1000°C. A hydrocarbon gas or carbon monoxide is a requirement for induction of CNT growth on the catalyst. In our system, we used thermal CVD with a resistively heated furnace.

In CVD, CNT growth based on diffusion models involves gas molecules, which decompose on the surface metal particles, and the resulting carbon diffuses into the catalyst [17]. Upon catalyst carbon saturation, carbon solute precipitates on the particle surface as crystalline graphite, forming a carbon nanotube.

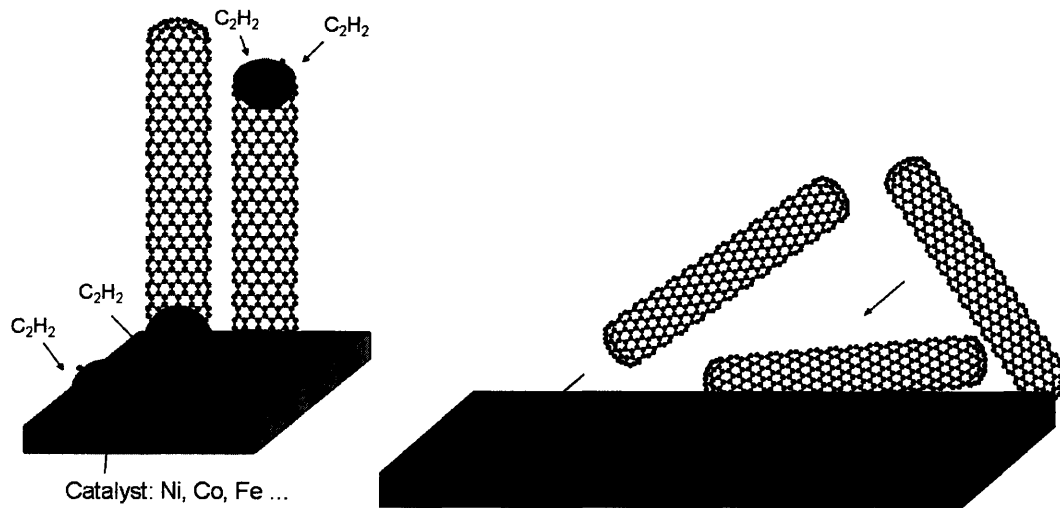


Figure 3. Assembly Methods [20]

Tip growth is seen with carbon from an acetylene hydrocarbon gas source (left). In tip growth, the catalyst floats on top of the CNT and in base growth the catalyst remains at the bottom. Carbon nanotubes may be grown separately and then place by chemical, field, or flow direction (right).

CNTs are generated through tip growth or base growth of the catalyst. During tip growth, the catalyst particles are detached from the substrate and move to the top of the growing CNTs, while in base growth, the catalyst stays at the base of the CNTs during growth, as shown in Figure 3. Tip growth is mostly seen with PECVD and with thermal CVD using catalyst-support powders. In contrast, base growth is seen with thermal CVD using catalysts on plain substrates [17]. Also, certain metal catalysts are specifically associated with either tip growth or base growth.

2.3 Hydrogen's Role in Pretreatment and During Growth

In the growth of carbon nanotubes, it is clear that hydrogen is an essential element having been implicated in a number of surface morphology changes of the catalyst. Wen et al. claimed that hydrogen treatment is a time dependent process, producing a number of different surface morphologies using a Co-Si catalyst [2]. With a long period of H₂

pretreatment, they showed that nanoparticles tend to agglomerate to reduce surface energy. However, initially the particles decrease in size before agglomerating into a larger one. Hence, there is a relationship between the particles with H₂ pretreatment and carbon nanotube growth, as low density of CNT occurs with no H₂ pretreatment. An optimal amount of H₂ pretreatment was also noted as too long a treatment started to decrease the yield of CNTs.

Another strong reductive gas NH₃ has been suggested to have a similar role as H₂. NH₃ pre-treatment may be a precursor for the growth of vertically aligned carbon nanotubes. Using a Co-Ni alloy catalyst, Lee et al. demonstrated that controlling the domain density of the catalyst by HF dipping and dry etching with NH₃ gas prior to growth was crucial in the growth of CNTs during CVD [4]. This process caused the carbon nanotubes to grow vertically due to steric hindrance of the CNTs. In the absence of NH₃ pretreatment, a low density of CNTs resulted; thus they concluded that both HF and NH₃ were necessary for vertical growth of CNTs. Since the reductive role of H₂ has been shown to be extremely important in the formation of carbon nanotubes, we evaluated this by time differences in H₂ exposure during annealing phase for our experiment.

The activity of hydrogen with the hydrocarbon gas has also been shown to be important. An optimal ratio of a hydrocarbon gas such as methane to hydrogen has been reported by Xiong et al [8]. They showed that methane molecules decompose during interaction with the catalyst particle surface, resulting in the dissolving of carbon into the catalyst. Then, the carbon has the option to diffuse onto the surface or through the catalyst particle, Fe-Mo, when supersaturation is reached. The growth of the CNTs

begins when precipitation of the carbon occurs on the surface, which is exposed to reactant gases. Xiong speculated that when the concentration of the carbon source, methane, is too high, there is an overabundance of decomposition and not enough precipitation, resulting in amorphous carbon and crystalline formation. Therefore, H₂ is essential for growth because it maintains the activity of the Fe-Mo catalyst. When H₂ is not present, CNT growth is stemmed and few CNTs grow, but when H₂ is supplied at an optimal ratio, the catalyst activates decomposition, diffusion, and precipitation, which optimize their growth rate. Hence, too much hydrogen tends to curb growth while too little hydrogen may not activate sufficient growth.

Though much research views H₂ favorably, not all literature points to H₂ as a beneficial gas in obtaining carbon nanotubes. Recently, Zhang et al. have shown that hydrogen radicals can be detrimental in the growth of carbon nanotubes when introduced with CH₄. In PECVD, using a Fe catalyst on a Si/SiO₂ layer, they showed that O₂ can spur growth and align SWNT vertically. Not only does O₂ affect CNT during the growth stage, it plays an extremely important role in the initial nucleation stage. In this study, H radicals may be etching the CNT, and a hydrogen rich environment may not favor SWNT growth. A PECVD system was utilized for their main results because a PECVD system can create many more hydrogen radicals. As a result, the differences in the effect of H₂ were more visible in the PECVD system than in the thermal CVD system.

2.4 Chemical State of the Fe Catalyst

Although thermal CVD has been investigated to a great extent, there is still a lack of knowledge on the exact chemical growth mechanism of CNTs. The catalyst chemical

state is believed to be one of the critical parameters in growth. For instance, Park et al. showed that Fe nanoparticles are easily oxidized to Fe_2O_3 after synthesis of CNTs, but they suggested that pure and liquid Fe is the actual chemical state of the catalyst during CNT growth [3]. Fe is reduced during growth due to the introduction of NH_3 but oxidizes into Fe_2O_3 during the cooling stage. They also noted that pure Fe is oxidized in normal atmospheric conditions, and the beginning state is almost always Fe_2O_3 . Furthermore, the inert gas, nitrogen, flown during the cooling phase may not have been inert and pure enough to prevent Fe oxidization after growth.

In another paper by de los Arcos et al. [5], they showed that one of the most important parameters in the growth carbon nanotubes is the catalyst and the catalyst-substrate interaction; therefore, the catalyst's chemical state becomes critical in the formation of the CNT type. Specifically, they addressed the state of Fe, FeO, and Fe_2O_3 as catalyst for nucleation of CNTs. Using in-situ XPS, de los Arcos determined that the chemical state of Fe in a Fe/ Al_2O_3 catalyst buffer system was Fe_2O_3 during annealing. After the CVD process, the catalyst changed to FeO. For catalyst morphology, they claimed that interaction between the substrate and the catalyst affected the morphology of the particle. Since the oxidation process at the interface of catalyst and alumina substrate was extremely strong, Fe mobility was severely curbed in the alumina buffer system. Therefore, the fact that the particles remained oxidized even after acetylene, C_2H_2 , was present showed that oxidation was strong, and that the Fe was chemically bound to the alumina substrate (Al_2O_3). de los Arcos tested three different substrate interactions: Al_2O_3 , TiN, and TiO_2 . Out of the three buffers examined, the original Fe catalyst particles were the smallest on the Al_2O_3 , resulting in a two times smaller diameter CNT

compared to the other two. On the TiO₂ and TiN buffer layers, FeO and Fe were the dominant catalyst states during annealing and after CVD. Hence, the oxidation state of Fe might be related to the size of the catalyst particle and the nanotube grown. FeO particles promoted a fast dense growth of thin CNTs, while Fe particles promoted MWNT growth with higher quality but less vertically aligned tubes. In our study, to monitor the chemical state of Fe, XPS was utilized to elucidate hydrogen's role in CNT growth.

To further the study of catalyst state on the growth of CNTs, recently SWNTs have been grown at temperatures as low as 350°C by CVD. Cantoro et al. showed that using C₂H₂ and NH₃ or H₂ facilitates the catalyst nanostructure of Fe and Al/Fe/Al prior to growth, allowing early nucleation of SWNT at a lower temperature. They concluded that catalyst surface is the most important factor in the formation of carbon nanotubes. The NH₃ or H₂ introduction “reduces initially oxidized Fe and facilitates surface mobility of metal atoms and clusters” [10]. In addition, NH₃ pre-treated catalysts were shown to have smaller catalyst diameters than vacuum annealed samples.

2.5 Chemical Morphology: Size

Finally, another parameter examined in our study that affects CNT formation was the catalyst morphology, especially its size. According to Homma et al. [6], there were noticeable differences in size when Fe catalysts and Fe₂O₃ catalysts of the same size were employed in the growth of CNTs. The Fe catalysts generated a mix of thick and thin CNTs, but the Fe₂O₃ catalysts generated thick carbon nanotubes. These differences were attributed to the size of the particle. The Fe was observed to agglomerate when viewed by AFM after CNT growth, but the Fe₂O₃ particles remained relatively small. They

claimed that the Fe particles tended to melt and agglomerate, creating larger particles than the original size of the catalyst. Hence, the non-agglomerating characteristic of Fe_2O_3 facilitates growth of thin CNTs.

In our study, to further elucidate the role of the catalyst in the growth process of carbon nanotubes, a thermal chemical vapor deposition (CVD) system was utilized to study the growth of CNTs on a $\text{Fe}/\text{Al}_2\text{O}_3$ catalyst substrate system. Two important considerations in the characteristics and the abundance of carbon nanotubes generated are catalyst and precursor gases utilized. Specifically, it has been shown that hydrogen pretreatment, the chemical state of the catalyst, and the morphology of the catalyst are extremely important. Hydrogen is utilized as a strong reductive gas in pre-treatment before growth is initiated, but its exact role has yet to be determined. Also, its effects on the catalyst chemical state and morphology are largely unknown.

As such, the goal of this experimental design is to demonstrate the effect of the timing of hydrogen gas introduction on the catalyst chemical state and morphology. We utilized a constant growth scheme of heating, annealing, and growing. By varying the introduction of hydrogen, clear differences in the chemical state of the catalysts, the morphology of the catalysts, and the type of CNTs, were produced. We found that hydrogen led to a morphology change that was quite different when introduced during the initial heating, the annealing, and the growth stages, leading to differences in nucleation and growth of CNTs. Scanning Microscopy (SEM) was used to monitor the quantity of CNTs by height of CNTs grown, Atomic Force Microscopy (AFM) to examine the catalyst morphology, and X-ray Photoelectron Spectroscopy (XPS) to determine the catalyst chemical state.

Chapter 3

Experimental Procedure

To determine the effects of H₂ on the growth of carbon nanotubes (CNTs), we relied on a catalyst system, which consisted 1 nm Fe deposited on 10 nm of Al₂O₃. These samples were prepared by electron-beam evaporation, in which Fe and Al₂O₃ were evaporated onto Si (100) substrate wafers. For the growth of carbon nanotubes, thermal chemical vapor deposition (CVD) was the chosen growth method, using H₂, C₂H₄, and Ar gases. From our previous studies, this set of gases produced dense growth of CNTs on this catalyst substrate system.

3.1 E-beam Evaporation

Using electron beam evaporation, a catalyst film with 10 nm of Al₂O₃ and 1 nm Fe was deposited using a Temescal VES-2550 with a FDC-8000 film deposition controller in a single pump down system. The substrates were 6-inch (100) silicon wafers (p-type, 1-10 cm, Silicon Quest International), which were cleaned by a "piranha" consisting of 3:1 H₂SO₄/H₂O₂ in solution. During the deposition, a quartz crystal monitor measured the film thickness, and after deposition the thickness was confirmed by Rutherford backscattering spectrometry (RBS). The Al₂O₃ was deposited by direct evaporation from a crucible of high-purity crystals.

3.2 CVD Furnace Arrangement

In the CVD chamber, the substrates with the Fe/Al₂O₃ catalysts were loaded

horizontally on an inclined sample holder, which was slightly inclined from the direction of the gas flow. The CVD chamber consisted of a quartz tube (3.5 cm in diameter) and a smaller inner quartz tube (2.25 cm internal diameter and 100 cm long) connected to the gas flows of Ar (99.9995%, Airgas), C₂H₄ (99.5%, Airgas), and H₂ (99.999%, Airgas), and was placed inside a high temperature furnace (Lindberg/Blue, model 59744-A, maximum temperature 1200°C, 31.5" length, 9" three temperature zones). The CVD system was equipped with three mass flow controllers (MKS 1179A) as shown in Figure 4.

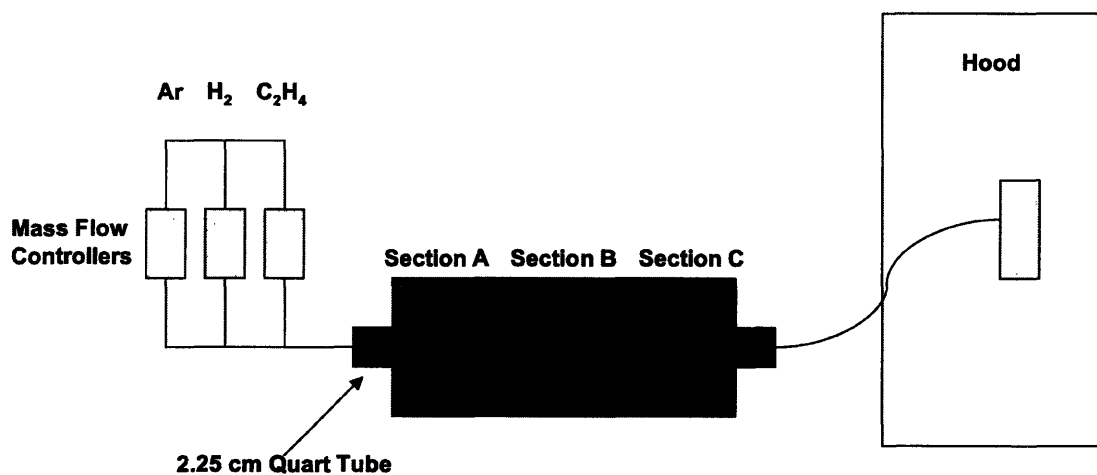


Figure 4. Experimental Setup of CNT Furnace Chamber. Ar, H₂, and C₂H₄ gas flows are controlled by automatic mass flow controllers and sent directly into the sealed quartz tube. There are three sections in the furnace, and the CNTs are grown in section C. All temperatures in the three sections are controlled by a central automatic system. Finally, gas exits the furnace and tube into a bubbler and then into a safety air flow hood. A low exit rate from the bubbler signals a leak in the system.

A thermocoupler was located in each of the furnace's three heating zones, called section A, section B, and section C. The samples were placed in section C, the last segment before gas flow exited the chamber. The placement of the sample in the chamber was to provide heated gases to the samples. The airflow exited into a liquid system in which the rate of flow could be calculated for consistency of all experiments.

3.3 CNT Growth Conditions

The independent variable, H₂, was introduced at a flow rate of 400 sccm at various time points throughout the temperature, annealing, and growth stages to compare the effect of H₂ on the catalysts of Fe/Al₂O₃. The catalysts on the Si wafer were cleaved into 0.5 cm x 0.5 cm samples for CNT growth. During the ramp stage Ar was flowed, and depending on the time of H₂ introduction, the combined total gas flow in the system was brought to a constant 600 sccm with Ar. 600 sccm was maintained during the temperature ramp for all experiments. After the temperature was ramped to 770°C, which took 40 minutes, the 15-minute annealing stage was started.

During the annealing stage, if H₂ was not introduced, the necessary gas flow changes were made to maintain a constant 600 sccm flow of gas with Ar. Finally, a 15-minute growth stage followed, when C₂H₄ was added to the chamber at a flow of 150 sccm. The total gas flow in the growth phase was 750 sccm. Ar was again used to maintain constant partial pressure. Then after completion of growth, the growth phase was discontinued by stopping the flow of H₂ and C₂H₄ and by cooling the furnace at room temperature. The Ar was reduced to 20 sccm after two minutes in order to gradually cool the system and remove the reactant gases. The different time points of H₂ introduction were the following: at the beginning of ramp, 200°C (4.5 minutes), 400°C (11.5 minutes), 600°C (21 minutes), start of anneal, 5 minutes after anneal, 10 minutes after anneal, 12 minutes after anneal, start of growth, 5 minutes into growth, 10 minutes into growth, 14 minutes into growth, 14.5 minutes into growth, and no H₂ introduction. A diagram of the hydrogen is shown in Figure 5. Two sets of all the trials were performed, one with the initiation of growth with C₂H₄ flow and one without exposure to C₂H₄ for morphology

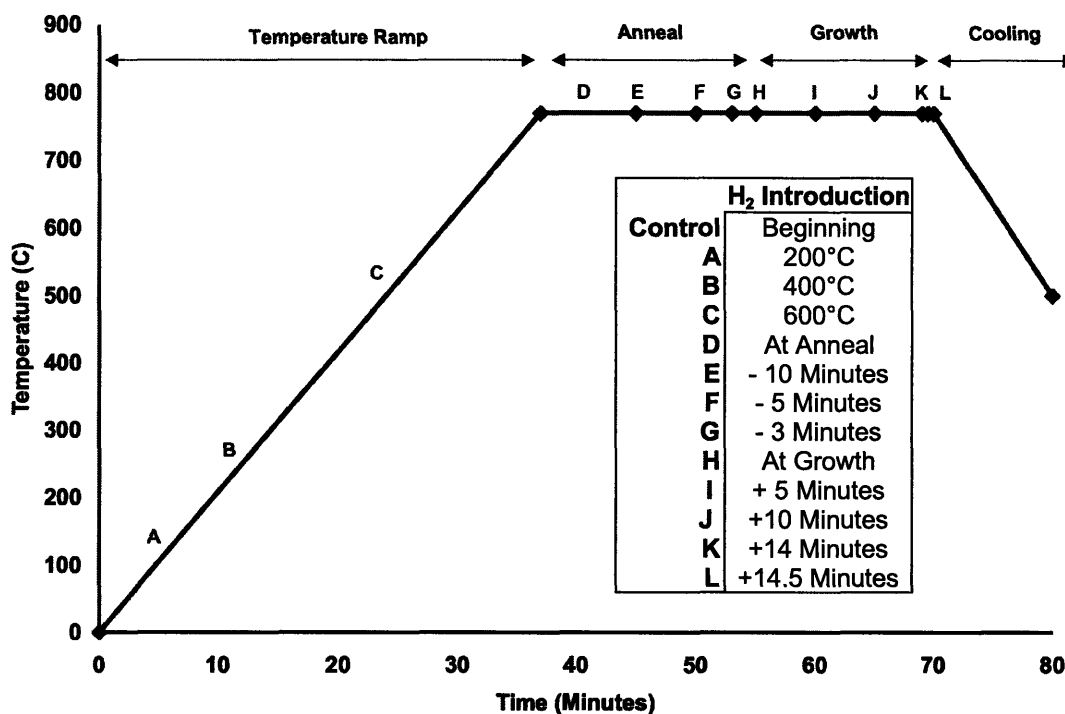


Figure 5. Experimental Design of Hydrogen Introduction

Hydrogen was introduced at the various points in separate experiments as indicated on the right. The flow of gases totaled 600 sccm, 600 sccm, and 750 sccm during the temperature ramp, annealing, and growth, respectively.

analysis of the catalyst by Atomic Force Microscopy (AFM). C_2H_4 , the hydrocarbon, is necessary to induce growth of CNTs.

3.4 CNT Analysis by SEM and Catalyst Morphology Analysis by AFM

The nanotubes were analyzed using scanning electron microscopy (JEOL 5910 and Phillips XL30 FEG-ESEM at around 5keV). The first SEM has a better resolution than the second: the first has <1.25 nm resolution when operating at 15KV and the second has a resolution of 3.5nm when operating at 30KV.

For analysis of the catalyst morphology, AFM (Digital Instruments Nanoscope IIIa / Dimension 3000 Scanning Probe Microscope) was used in tapping mode on the second

set of samples prepared without C_2H_4 exposure. The spring constant was 40 N/m with a resonance frequency of 300 kHz.

3.5 Catalyst Chemical State Analysis by X-ray Photoelectron Spectroscopy (XPS)

For analysis of the chemical state of the catalyst, the samples were prepared over a course of two days and analyzed immediately in XPS. There were two sets of experiments for XPS analysis. One set was used for analysis of the catalyst's surface before induction of growth by C_2H_4 . Hence, this set was cooled rapidly by moving the sample out of the furnace after the 40 minute temperature ramp stage and the 15 minute annealing stage. The second set of samples was used to examine the chemical state of the catalyst after the conclusion of the entire CNT growth process. However, C_2H_4 was not introduced to any of samples for XPS during growth, as the presence of C_2H_4 would have caused CNTs to cover the substrate. Ar was used to keep constant partial pressures in the absence of C_2H_4 .

The first set of samples prepared for XPS examination, which were cooled rapidly at the beginning of the growth stage, included the following: Ar only, 400°C H_2 introduction, and -15 minutes to growth H_2 . The second set, which were cooled slowly at the end of the CNT growth process, included the following: Ar only, 400°C H_2 introduction, -15 minutes to growth H_2 introduction, and H_2 introduction at growth. A Fe/ Al_2O_3 sample, untreated by heat or reactant gases, was used a control.

An Axis Ultra X-ray Photoelectron Spectrometer (Kratos Analytical) was used for XPS. The energy position of each spectrum was calibrated with reference to the 1s level of carbon with a binding energy of 285eV. A monochromatic Al K-alpha source with a

spectral resolution of 160eV was used to examine the chemical state of the catalyst.

Chapter 4

Results

4.1 Scanning Electron Microscopy Elucidates the Effect of H₂

To determine the interaction of H₂ with the catalyst, Fe/Al₂O₃, for initiating carbon nanotube growth, we examined the growth of CNTs using SEM. A sample with no H₂ during the entire ramp, anneal, and growth stages was used as a negative control. A sample with H₂ present during the entire process was used as a positive control. It was observed that negative control grew a very thin layer of tangled CNTs, as shown in Figure 6a and 6b, while the positive control acquired clear covered growth of ~.3mm vertical CNTs on the substrate, as shown in Figure 6c and 6d.

H₂ Introduction during Temperature Ramp

As the temperature ramp process was continued for different samples, H₂ was introduced at 200°C, 400°C, and 600°C, as shown in Figure 7. These temperatures were reached at 4.5, 11.5, and 21 minutes into heating, respectively. When H₂ was introduced at 200°C, very little growth was achieved and the substrate was bare to the naked eye. As the H₂ was introduced at 400°C and 600°C, the growth was curbed with very little CNTs resulting on these samples. When H₂ was introduced at 600°C, CNTs were seen only on the edges of the substrate.

H₂ Introduction during Annealing

For H₂ introduction analysis during annealing, the different samples were introduced to H₂ at -15, -10, and -5 minutes prior to growth as shown in Figure 8. The

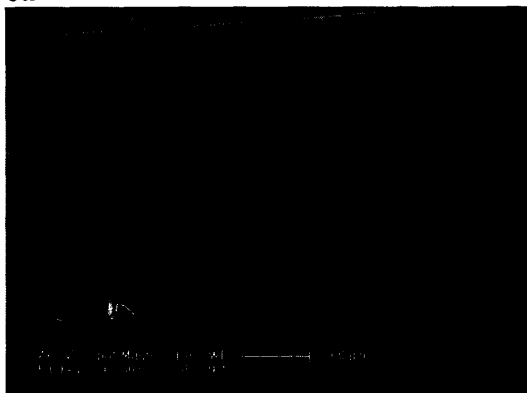
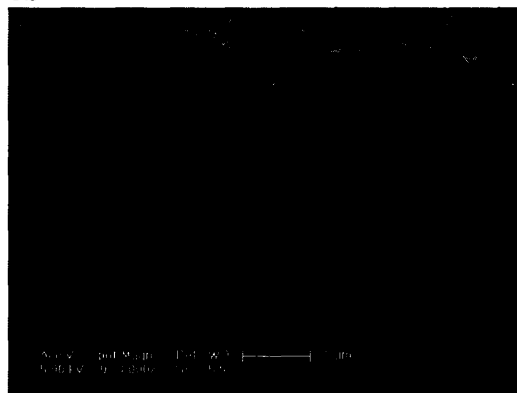
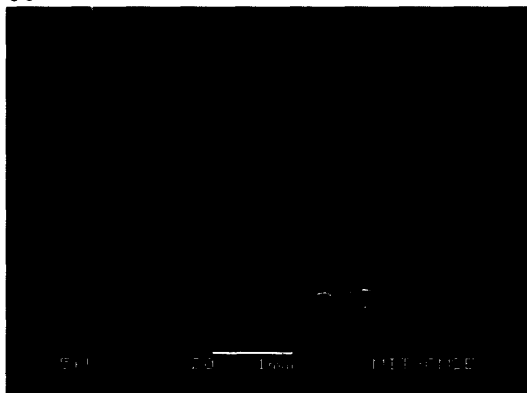
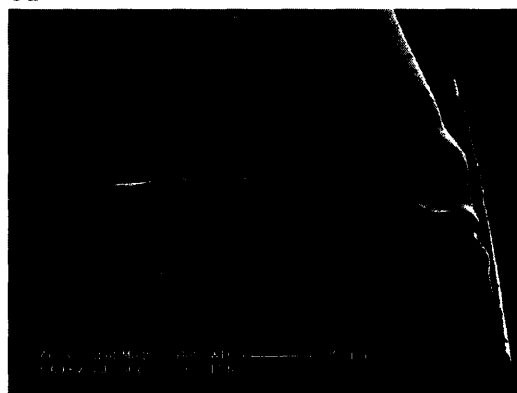
6a**6b****6c****6d**

Figure 6. SEM Images of CNTs Resulting from Control Conditions.

a-b) A extremely thin layer of tangled CNTs were present when H_2 was not introduced. c-d) Carbon nanotubes were present in a dense “forest” formation when H_2 (150 sccm) was present from initial heating and during whole the ramp, anneal, and growth stages.

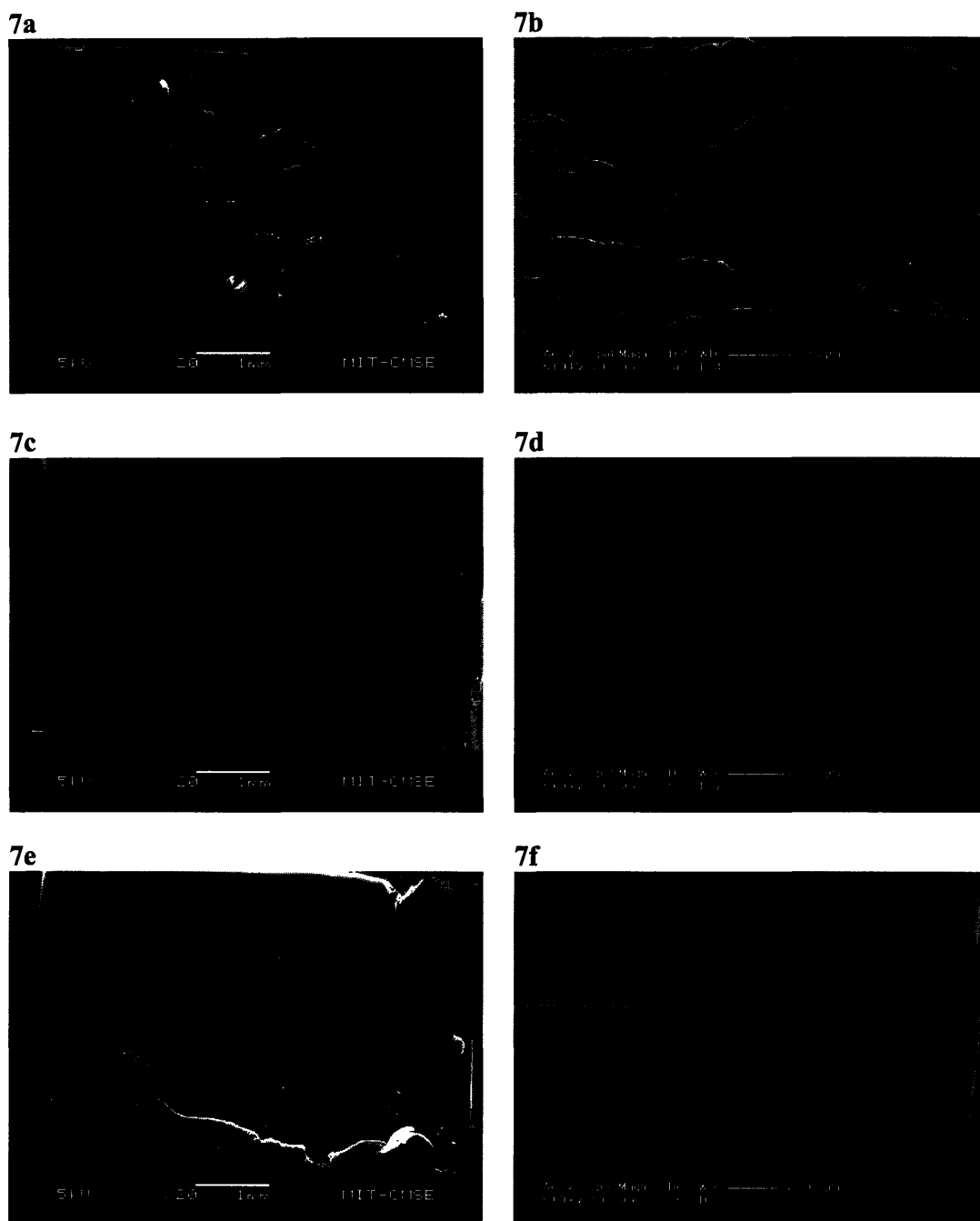


Figure 7. SEM of CNTs when H₂ was introduced during temperature ramp.
 a-b) Carbon nanotubes were sparsely seen when H₂ was introduced at 200°C (4.5 minutes) during temperature ramp. c-d) When H₂ was introduced at 400°C, the original Si wafer was still clearly visible as minimal CNT growth occurred. d-f) When H₂ was introduced at 600°C, the center of the substrate did not show much CNT growth while the edges showed vertical growth of CNTs.

resulting growth of CNTs at -15 minutes H₂ introduction was similar to the CNTs grown when H₂ was introduced at 600°C during temperature ramp with growth predominantly on the edges of the substrate, but with CNTs on the edges and “islands” of CNTs in the center. For H₂ introduction at -10 minutes prior to growth (5 minutes into anneal), a clear change was observed as the CNTs grew to longer lengths and covered the substrate. H₂ introduction at -5 minutes prior to growth (10 minutes into annealing) showed a clear carpet of uniform CNTs at a height of ~ 0.3mm.

H₂ Introduction during Growth

With the introduction of H₂ at the beginning of growth, initiated by C₂H₄ introduction, a “dense carpet” of CNTs formed as shown in Figure 9. To summarize thus far, the growth pattern has gone from covered growth of CNTs to sparse growth to recovery of covered CNT growth on the substrate with delayed H₂ introduction. H₂ introduction at -10 minutes prior to growth was the time point at which growth of CNTs recovered. However, when H₂ was introduced 5 minutes into growth (the catalyst had been exposed to C₂H₄ for 5 minutes), the substrates showed remarkable growth as the height of the CNTs was ~0.5mm and almost completely covered the substrate. In addition, two types of CNTs were observed. On the outer edges of the sample, the CNTs were similar to CNTs grown with no H₂ as in Figure 6a and 6b. In the center, much longer vertical CNTs were visible. Also, at the top of the CNTs in the center of the substrate, a two-layer system developed with a different layer of CNTs analogous in length and characteristics to those on the outer edges, implicating that the growth at the top of this two-layer system occurred when only C₂H₄ was present. 10 minutes after C₂H₄ was introduced, H₂ flow caused vertical growth of CNTs to lengths of ~0.9mm.

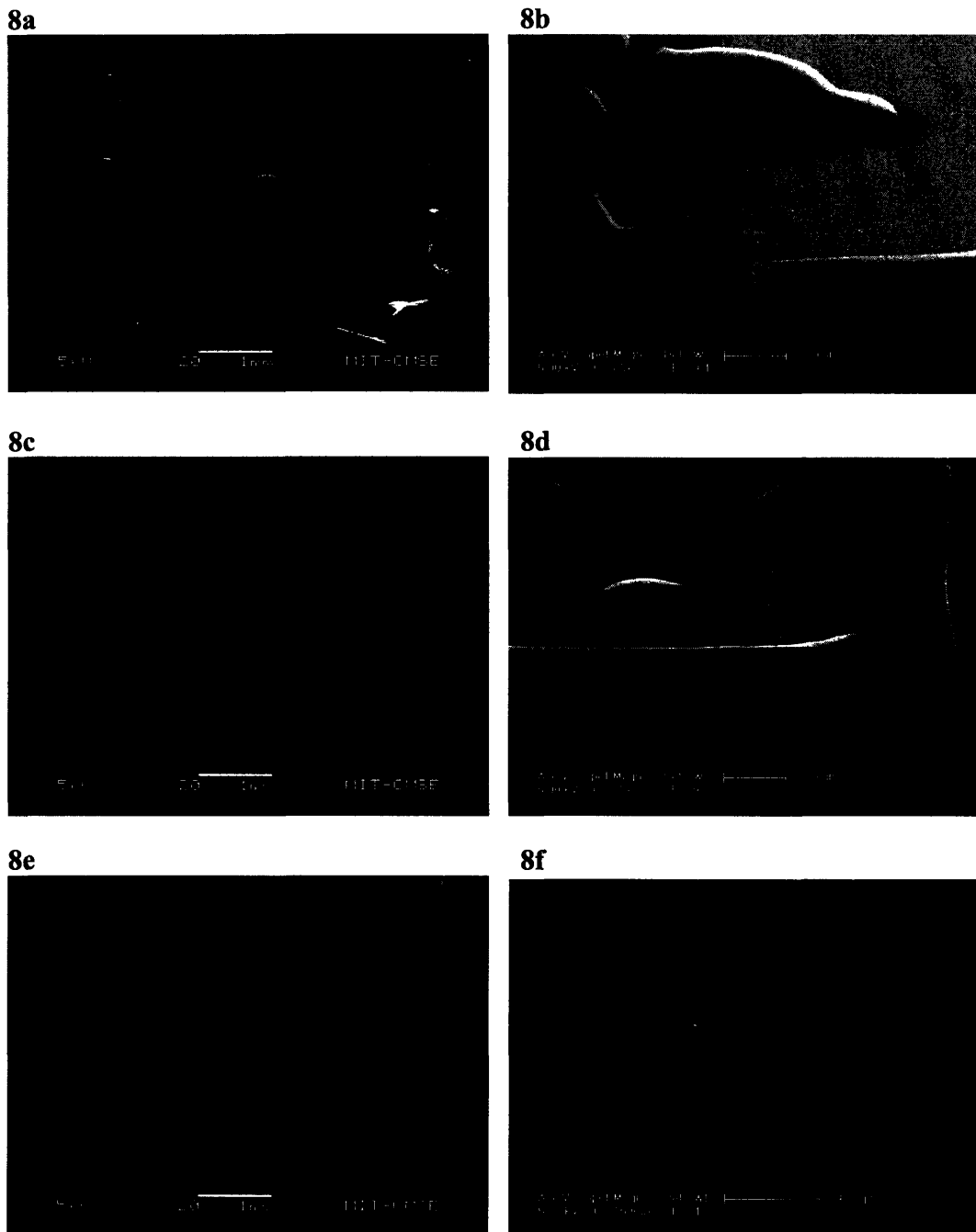


Figure 8. SEM Images of CNTs when H₂ was introduced during the 15 minutes of annealing.
 a-b) When H₂ was introduced at the beginning of annealing (-15 minutes from growth initiation), similar results were seen as with Fig. 3e and 3f. Growth of CNTs was seen on the outer edges but was minimal in the center of the sample. c-d) When H₂ was introduced -10 minutes from growth initiation, the outer edges had the same degree of CNT growth, but the center began to show the some “denser” growth. e-f) H₂ introduction 5 minutes prior to growth showed a recovery of growth as the substrate was almost clearly covered with CNTs.

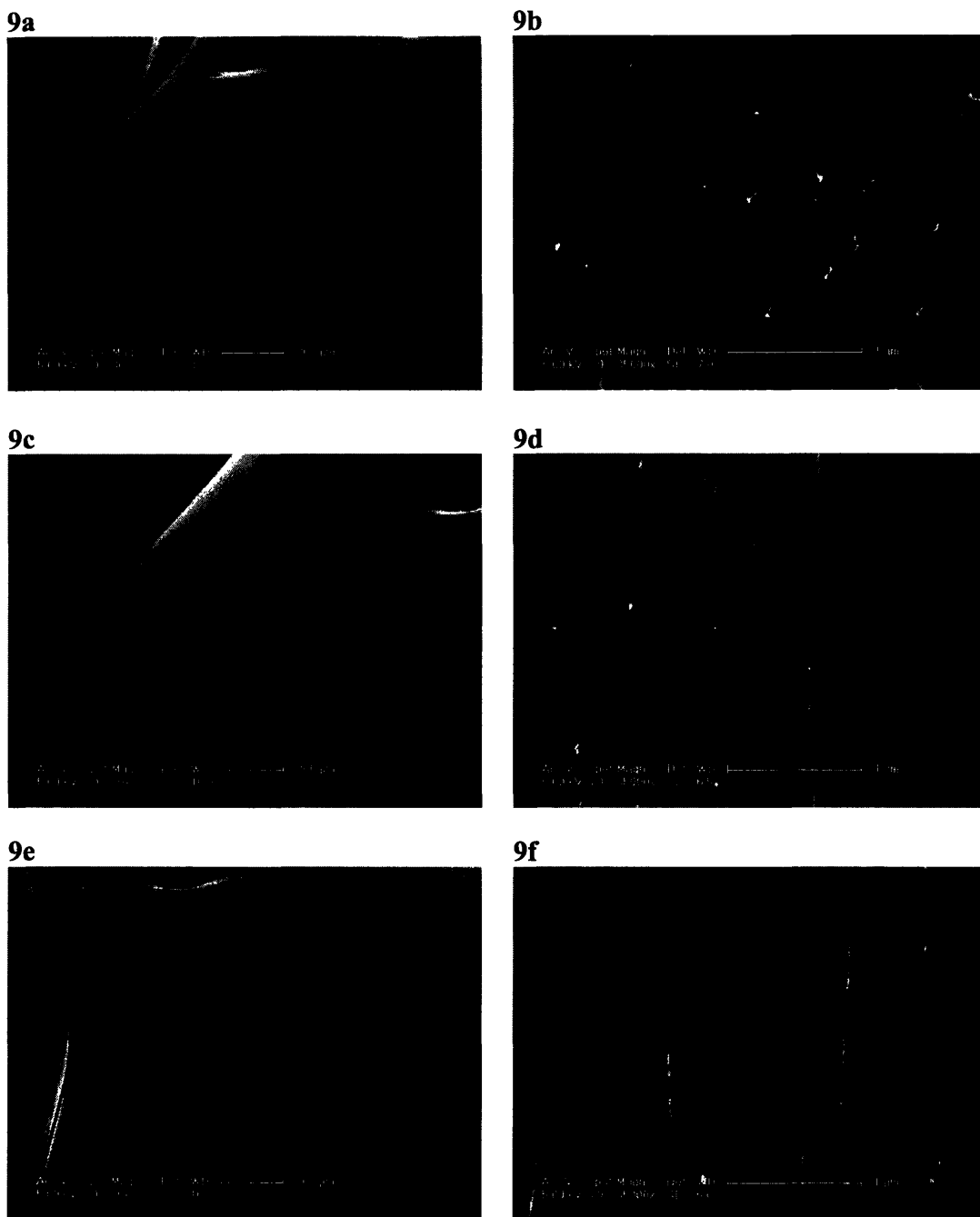


Figure 9. SEM of CNTs when H_2 was introduced during the growth stage.
 a-b) H_2 introduced at growth with C_2H_4 showed clear growth of CNTs. c-d) When H_2 was introduced 5 minutes into growth, longer CNTs were observed and the CNTs were more vertically aligned than when H_2 was introduced at the beginning of growth. e-f) H_2 introduced 10 minutes into growth showed extremely vertically aligned CNTs and the longest CNTs grown in this study were observed.

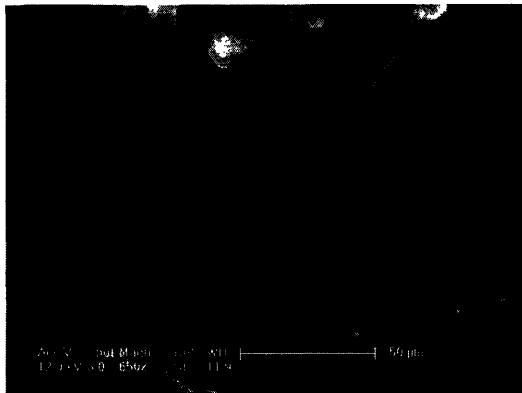
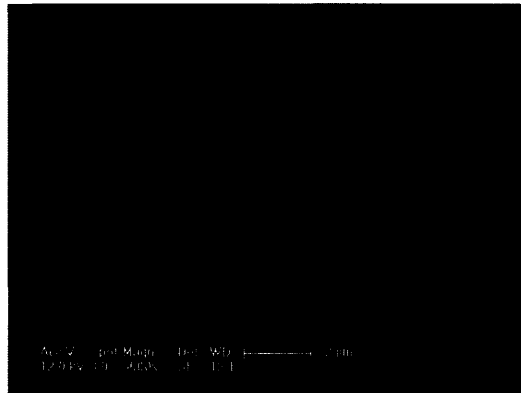
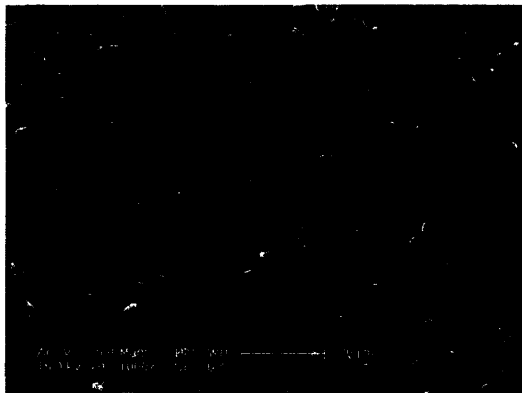
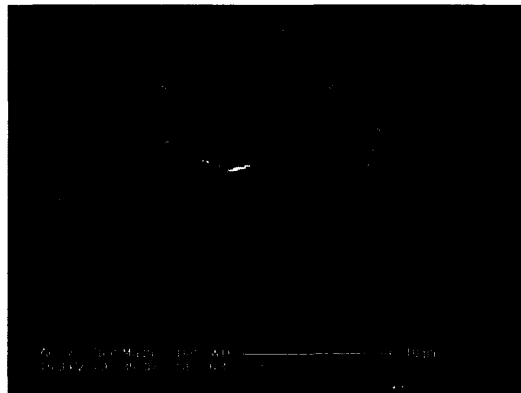
10a**10b****10c****10d**

Figure 10. SEM CNTs exposed to 1 minute and 30 seconds of H₂.

a-b) At 14 min into growth, H₂ was introduced, and a similar carpet was seen as in Figure 2a and 2b. However, in this Figure, there were bundles of CNTs, which had rapid growth. Even within the 1 minute of H₂ exposure, remarkable height differences occurred. c-d) At 14.5 minutes, H₂ was introduced for 30 seconds and similarly as seen in Figure 6a, CNTs started to grow at extremely fast rate as evidenced by the longer bundles of CNTs dispersed throughout the substrate.

Compared to the samples exposed to H₂ 5 minutes into the growth stage, the samples introduced to H₂ 10 minutes into the growth stage did not have an outer layer of very thin CNT growth.

In order to further analyze the effects of the H₂ during growth, H₂ was introduced for 1 minute and 30 seconds in separate experiments prior to the completion of growth, as shown in Figure 10. Even with only 1 minute of H₂ exposure, CNTs with lengths of ~0.2mm in certain areas were seen, distributed almost evenly throughout the substrate. The 30 seconds of H₂ flow showed that even 30 seconds of H₂ can have remarkable catalytic type of an effect. “Pillars” of CNTs were seen growing from a very thin layer of CNTs.

We found two effects of H₂: when H₂ was not introduced at the beginning of heating but was introduced during temperature ramp or annealing, the CNTs growth was not optimal. When H₂ was introduced close to the growth phase, then there was recovery in the growth of CNTs. The complete results are summarized in Figure 11. In order to correlate these results with catalyst morphology, we examined the catalysts at the same time points without introduction of C₂H₄, which induces growth of CNTs.

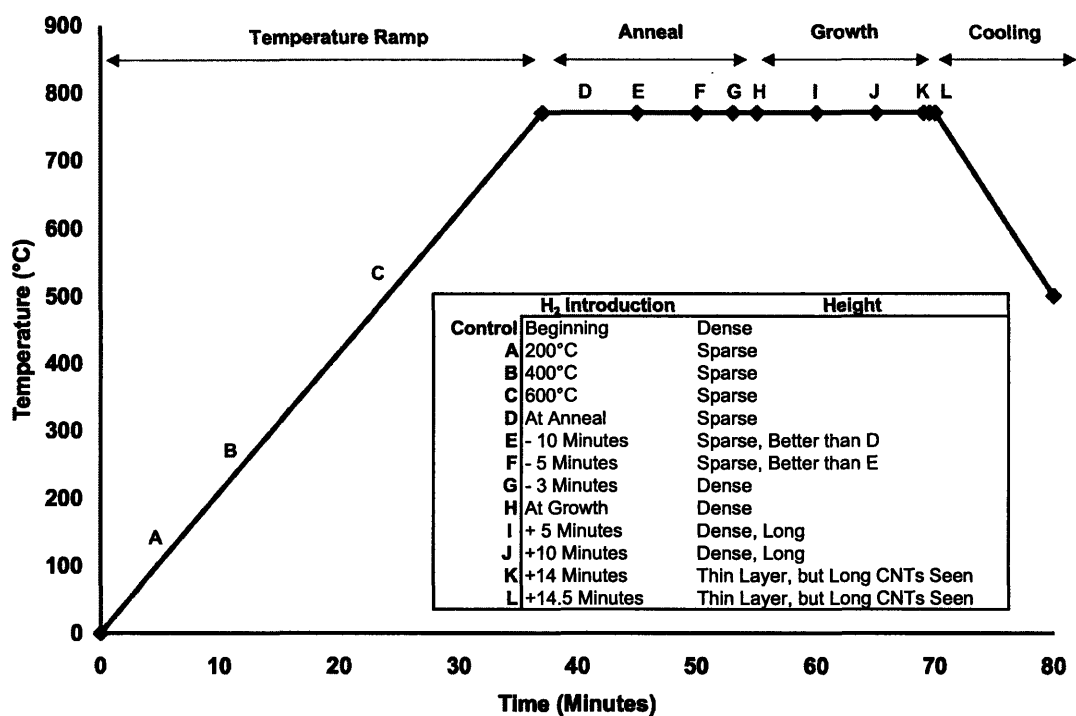


Figure 11. Experimental Conditions and CNT Growth Results

Growth was extremely dense when H₂ was introduced at the very beginning and was in a period of sparse growth with H₂ introduction during temperature ramp and annealing. When H₂ was introduced at growth with C₂H₄ or later during growth, long vertically aligned CNTs were observed.

Table 1. Summary of the CNT Heights

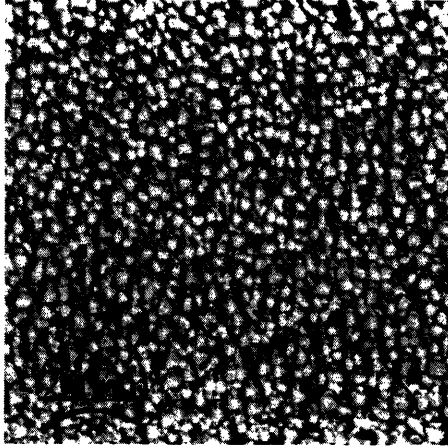
	H ₂ Introduction	Height (mm)
Control	Beginning	~0.3
A	200°C	-
B	400°C	-
C	600°C	-
D	At Anneal	Edges ~0.3
E	- 10 Minutes	~0.3
F	- 5 Minutes	~0.3
G	- 3 Minutes	~0.3
H	At Growth	~0.3
I	+ 5 Minutes	~0.5
J	+10 Minutes	~0.9
K	+14 Minutes	< 0.1
No H ₂	-	< 0.1

4.2 Catalyst Morphology by AFM

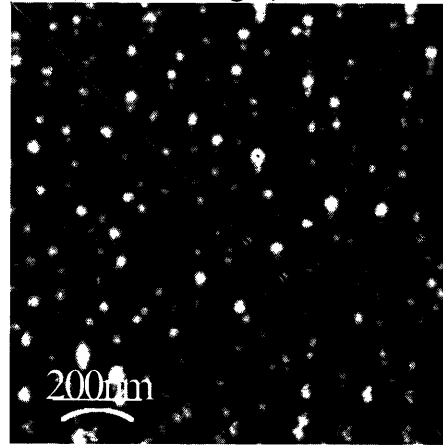
H₂ Effect on Catalyst Morphology

The effects of H₂ on catalyst morphology can be seen in Figure 12. When the catalysts were introduced to H₂ early during the temperature process at 200°C, the catalyst particles were seen at a high density as shown in Figure 12a and 12b. However, as H₂ was introduced later, at -15 minutes prior to growth, fewer catalyst particles were seen but were larger in general than those with early introduction to H₂, as shown in Figure 12c and 12d. When H₂ was introduced even later at the induction of growth, fewer catalyst particles were seen but were larger in general, as visible in Figure 12e and 12f. A summary of the results is shown in Figure 13. Hence, long exposure to H₂ caused reduction of the Fe catalyst, resulting in nucleation into smaller particles and a higher density of such particles in AFM analysis. Also, when H₂ treated catalysts were compared to those, which had not been treated to H₂, a large difference was observed (Not Shown). Without any introduction to H₂, the catalysts on substrate were relatively smooth and flat. In order to assess for Al₂O₃ morphology changes, the bare Al₂O₃ (15nm on Si) substrate was also viewed by AFM. These surfaces were relatively smooth, and there was little variation in height, allowing us to conclude that Fe, not Al₂O₃, particles exhibit morphology change (Not Shown).

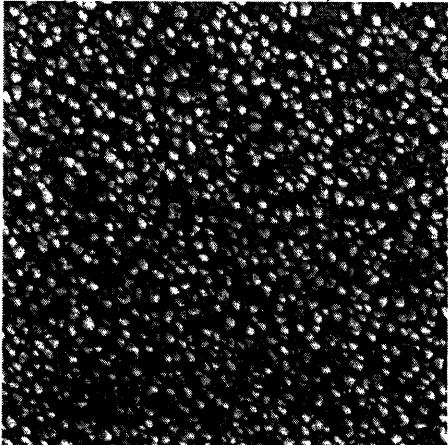
12a (200°C - Phase)



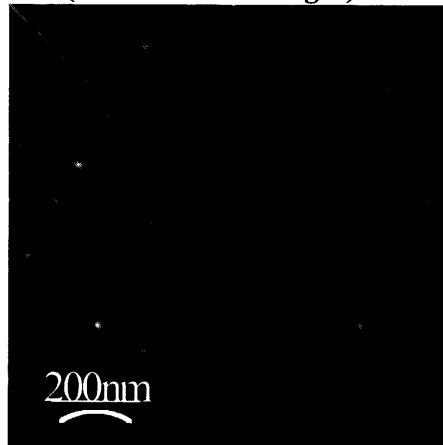
12b (200°C - Height)



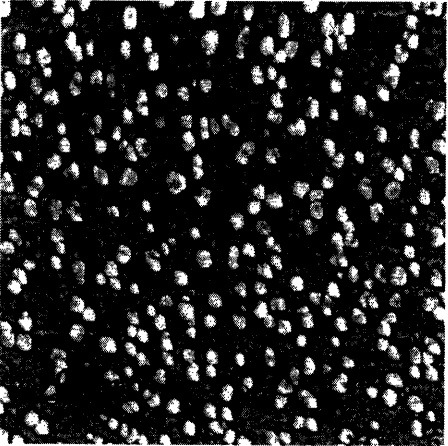
12c (-15 Minutes - Phase)



12d (-15 Minutes - Height)



12e (At Growth - Phase)



12f (At Growth - Height)

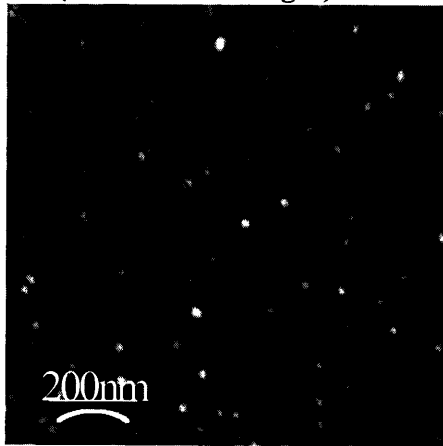


Figure 12. AFM of Fe/ Al₂O₃. a) H₂ introduction at 200°C - Phase b) H₂ introduction at 200°C – Height c) H₂ introduction at -15 minutes - Phase d) H₂ introduction at -15 minutes – Height e) H₂ introduction at growth - Phase f) H₂ introduction at growth – Height. As the exposure to H₂ was longer, the samples had a higher density of particles. In addition, the particles were smaller in diameter. Scan Size – 1 μm x 1 μm

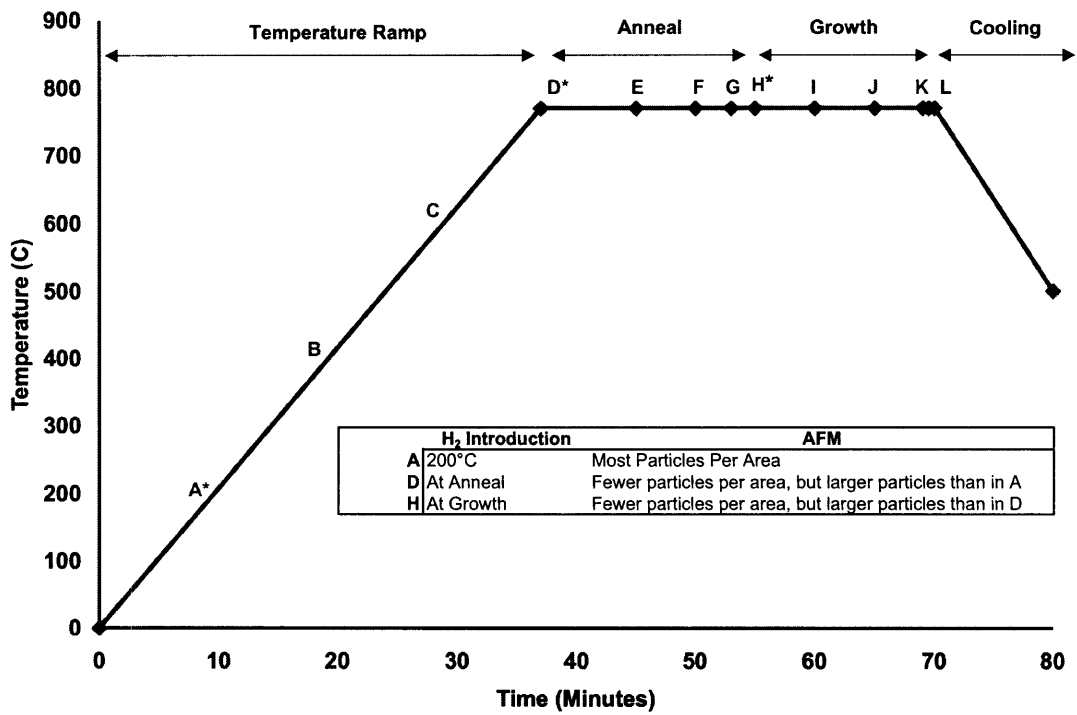


Figure 13. Summary of AFM of Fe/ Al₂O₃. As the exposure to H₂ was longer, the samples had a higher density of particles, but the particles were smaller in diameter.

CNT Growth Inducible by Catalyst Morphology

In order to establish a relationship between morphology and growth of CNTs, the catalysts which were exposed to H₂ at 600°C, were examined. On these samples, growth was observed only on the edges of the sample, but not in the center. To confirm these findings, AFM was used to examine the morphology at the edges and at the center. The results showed that on the edges, the catalysts have a rough surface with visible differences in height as shown in Figure 14c and 14d, while the center of the catalyst had a much more periodic and smoother surface with heights ranging over a couple of nanometers as shown in Figure 14e and 14f. Figure 14c and 14d were compared to Figure 14a and 14b, which exhibited dense growth, as shown in Figure 9c and 9d.

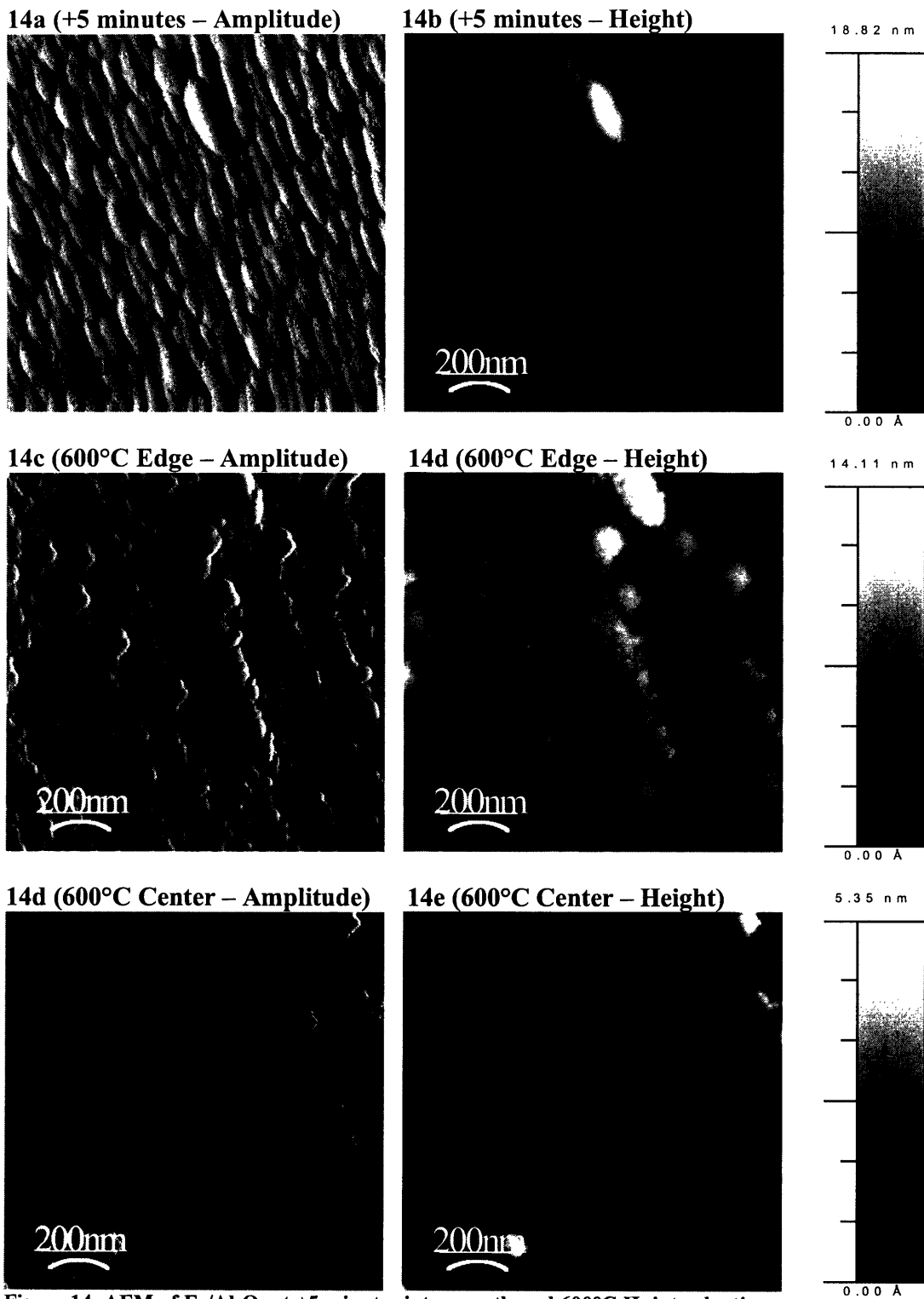


Figure 14. AFM of Fe/Al₂O₃ at +5 minutes into growth and 600°C H₂ introduction.
 a-b) +5 minutes H₂ introduction showed a morphology for CNT growth. c-d) At the edge of the samples, where growth of CNTs was seen, there was a clear difference in the catalyst morphology. d-e) In the center, the sample was smooth and roughness was minimal, but on the edges, there was surface roughness and variation in height. Hence, growth was initiation on rough surfaces with variations in catalyst height.

4.3 Chemical State of Catalyst by XPS

In Figure 15, a significant change in the chemical state of the Fe and Al₂O₃ of the catalyst can be followed. XPS analysis of the reference catalyst showed a binding energy (BE) of 75.4eV at the Al 2p 3/2 peak and 711.2eV at the Fe 2p 3/2 peak, indicating that Fe began the CNT growth process as an oxidized Fe due to atmospheric presence of oxygen. The Fe corresponding to 711.2eV is primarily a mixture consisting of Fe₂O₃ alpha (711eV) and Fe₃O₄ (711.1eV), or FeOOH (711.15eV). For the state of Al₂O₃, the initial binding energy was 75.4eV. This higher binding energy indicates that it may be a combination of AlO_x / Al₂O₃.

Fe and Al₂O₃ after CNT Growth Cycle Completion

To examine the effects of H₂ introduction on the catalyst's chemical state at the end of the CNT growth cycle, the samples were cooled slowly analogous to protocols used to grow CNTs but without C₂H₄. The results, in Figure 15, indicate that the chemical state of Al₂O₃ changed according to the time of H₂ introduction. With H₂ introduction during temperature ramp, a large decrease in binding energy from 75.4eV to 74.5eV was observed. When H₂ was introduced at -15 minutes prior to growth (at the beginning of annealing), the binding energy of Al changed from 74.5eV (400°C) to 74.2eV, corresponding to Al₂O₃. With later introduction of H₂ at growth (74.3eV) and no H₂ introduction (74.4eV), there was only a slight change in binding energy when examining the binding energies of the catalysts.

For the Fe particle, an increase in BE was seen as a result of reduction. Early introduction of the H₂ changed the catalyst chemical state. However, a decrease in

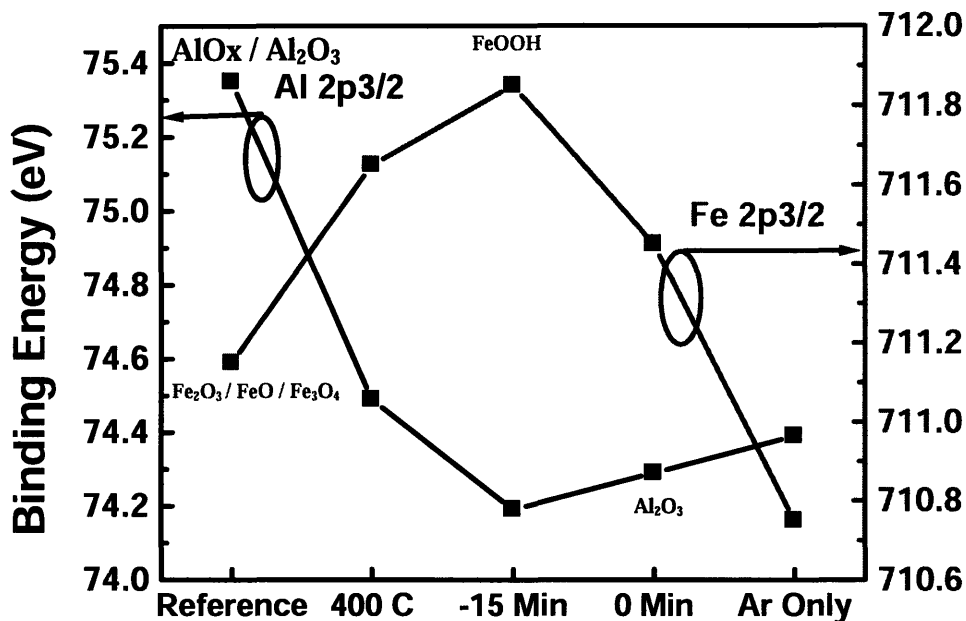
binding energy was also seen when H₂ was introduced later than -15 minutes to growth. This could have been a result from limited exposure to H₂.

Fe and Al₂O₃ after Annealing

For the catalysts which were fast cooled to examine the chemical state of the Fe prior to initiation of growth, a similar trend was seen. There is an increase in binding energy examined at Fe2p_{3/2} with decreasing exposure time to H₂. The largest change was detected between the temperature ramp and the annealing phase introduction of H₂. When H₂ was introduced at -15 minutes to growth, the binding energy was 711.7eV at the Fe2p_{3/2} peak, corresponding to FeOOH and when H₂ was introduced at 400°C, the peak corresponded to Fe₃O₄ at 711.1eV. The catalyst with no H₂ exposure had a slightly lower binding energy of 711.6eV than the sample exposed for 15 minutes. For examination at Al2p_{3/2}, the opposite change in binding energy was observed, compared to Fe, as binding energy decreased when H₂ was introduced during temperature ramp. The binding energy examined at Al2p_{3/2} when H₂ was introduced at 400°C was 75.2eV, corresponding to AlO_x, and when introduced -15 minutes prior to growth, the peak corresponded to Al₂O₃ at 74.3eV.

The catalyst state examined prior to growth (fast cooled) and after growth (slow cooled) had the same binding energy of 74.3eV for Al. For Fe, the measured binding energies were 711.6eV and 711.5eV for fast cooled and slow cooled, respectively (Figure 16). The similar binding energies of Fe at growth (fast cooled and slow cooled) showed that the different types of cooling and the additional 15 minutes exposure to H₂ for catalysts, which had not been introduced to H₂ before the growth period, did not affect the catalyst chemical state significantly.

15a) Slow Cooled – Catalyst after Growth Period



15b) Fast Cooled – Catalyst before Growth Period

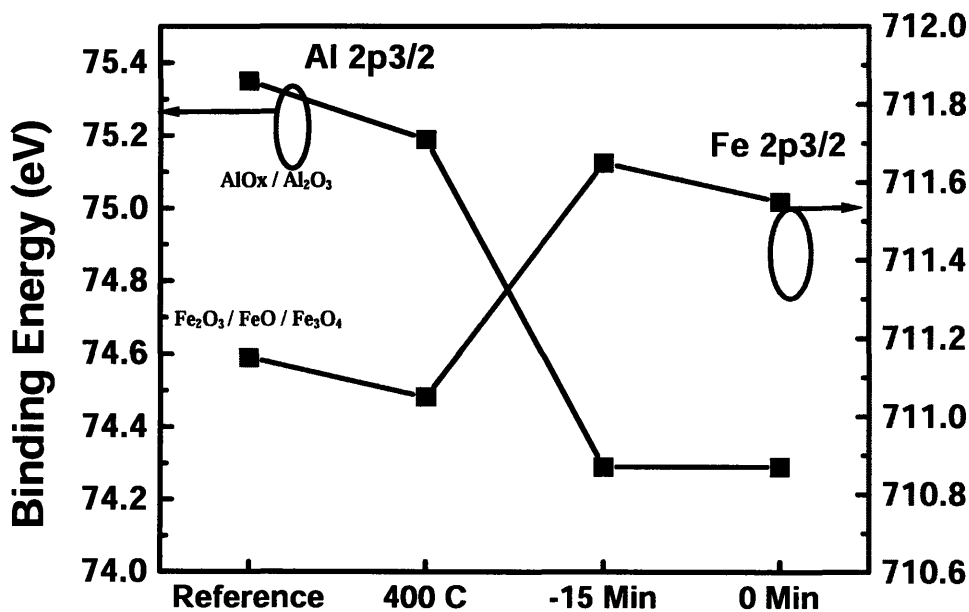


Figure 15. XPS of the Fe/Al₂O₃

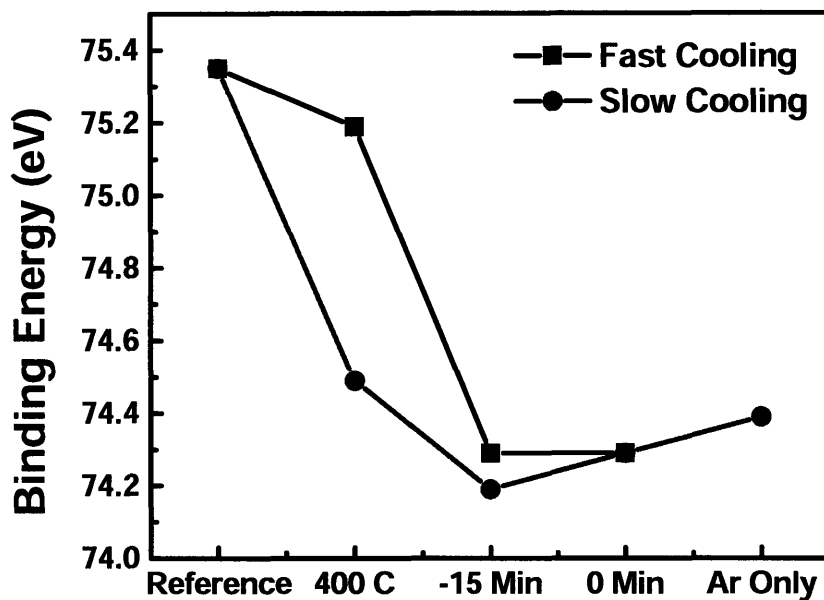
a) Examination of the catalyst at the end of the CNT growth period, which was slow cooled. b) The catalyst at the beginning of the growth time period. A clear change in BE is seen as Fe is reduced.

H₂ Introduction during Temperature Ramp and Annealing

Differences were detected in the 400°C and -15 minute samples due to the additional 15 minutes of heating and exposure to gases during the growth stage. For the chemical state of Al, we saw that that samples which were fast cooled, did not decrease in binding energy as rapidly as the samples which were slow cooled, as shown in Figure 12. For Fe, though the general trend of increase in binding energy was similar for both fast and slow cooled samples, when the samples were viewed before growth, they did not have the same magnitude increase in binding energy. The binding energy at 400°C H₂ introduction corresponded to Fe³⁺ / Fe₂O₃ before the growth phase, but at the end of growth, the chemical state of the Fe was FeOOH, indicating that greater reduction had occurred. In addition, analogous results were seen at -15 minutes, but the differences in binding energies were smaller than at 400°C H₂ introduction because fast cooling had a BE of 711.9eV and slow cooling 711.7eV. These chemical states both corresponded to FeOOH.

For the Al peak analysis, similar results were also seen. At 400°C H₂ introduction, there was a large difference in the state of the sample before the 15 minute growth period and afterwards. The difference in binding energies became much smaller in the -15 minutes introduction samples and was minimal when H₂ was introduced at growth. At 400°C H₂ introduction, the catalyst had a BE of 75.2eV (AlOx) before growth (fast cooled) and a BE of 74.5eV (Al₂O₃) after growth (slow cooled). At -15 minutes introduction, the BE before growth and after growth was 74.3eV and 74.2eV, respectively. Both binding energies corresponded to Al₂O₃.

16a) Al2p3/2



16b) Fe2p3/2

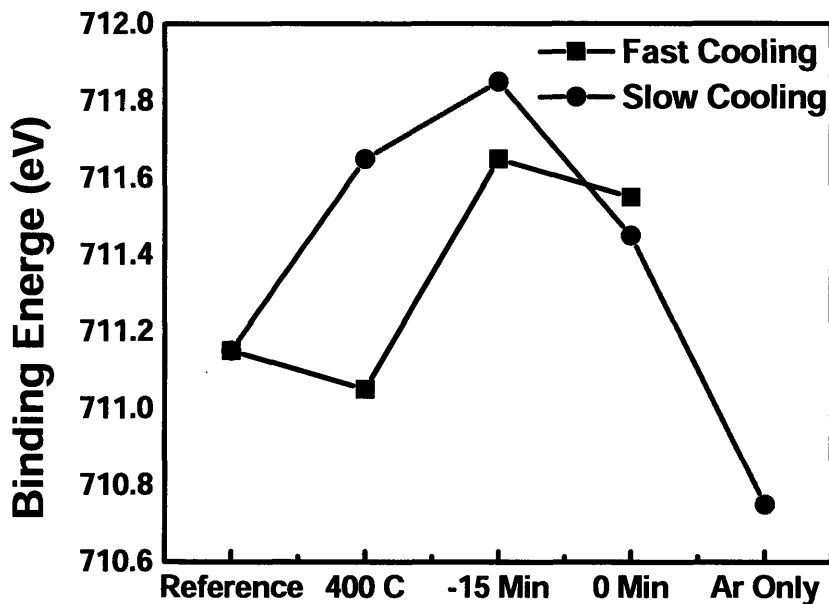


Figure 12. XPS of the Fe/Al₂O₃. Comparison of catalyst before and after growth.
 a) For Al, there was a decrease in BE as the Al on the surface was seen to change from a mixture of AlOx / Al₂O₃ to pure Al₂O₃. b) For Fe, an increase in BE was seen with the reduction by H₂. In addition, both chemical states were the most different during H₂ introduction at 400 C and -15 minutes.

The XPS data showed a significant reduction of Fe as H₂ was introduced. The differences became larger when H₂ exposure was longer on the catalyst. Most importantly, the large change in chemical state between 400°C and -15 minute exactly correlated to time points when CNT growth was hindered. Hence, there is a clear relationship between the catalyst morphology, the chemical state, and the resulting CNT growth.

Chapter 5

Discussion

By varying the time of hydrogen introduction, we have shown that the Fe catalysts, which induce growth of CNTs, exhibit different morphologies and chemical states. Therefore, we propose a preliminary model for the growth of carbon nanotubes on a metal catalyst based on these results.

5.1 CNT Growth Examined by SEM

First, the state of the Fe catalyst is extremely important in achieving carbon nanotube growth. With changes in the time of H₂ introduction, there were catalyst differences in morphology and chemical state, which consequently resulted in lower yields of CNTs with H₂ introduction during temperature ramp and higher yields of CNTs with H₂ introduction during growth. When H₂ was present from the beginning of growth, AFM and XPS analysis confirmed that the Fe catalyst was morphologically and chemically distinct than when H₂ was introduced during each of the three stages of CNT growth: temperature ramp, annealing, and growth initiated by C₂H₄.

SEM analysis of the CNTs when H₂ was introduced for one minute and 30 seconds just before end of the growth cycle confirmed that H₂ is a crucial element for rapid growth of carbon nanotubes. Even with such short periods of exposure to H₂, “columns” of carbon nanotubes were observed as shown in Figure 10a and 10b. The thin layer of CNTs beneath the “columns” on these substrates exactly resembled the CNT growth with no H₂ exposure. Hence, we believe that H₂ may play a role in optimizing the rate of carbon decomposition, diffusion, and precipitation in the formation of a carbon

nanotube. It has been reported by Xiong et al. that an optimal ratio of H₂ to hydrocarbon gas exists [8]. Hence, the presence of H₂, even for such short periods, optimized the ratio of H₂:C₂H₄ resulting in rapid growth. This phenomenon could be addressed with future experiments by changing the amount of H₂ introduced during these short periods.

5.2 Catalyst Morphology

In our study by AFM analysis, we observed that increasing the time of H₂ exposure caused the catalyst particles to become smaller and more distinct so that the particle densities per unit area were increasing. Changes in the height of the catalysts were also observed when compared to catalysts without heat or gas treatment. If a one to one correlation between a catalyst particle and a CNT were assumed in the context of a diffusion based growth model suggested by Kanzow [19], these smaller particles should have catalyze more CNTs, since the carbon simply would have had a shorter path length for diffusion. However at 400°C H₂ introduction, the smaller particles were present in high density but did not catalyze growth of many CNTs or very long CNTs (~.3mm for H₂ from the beginning). Based on these results, we can rule out particle size dependence in the diffusion model. However, we did notice significant differences in the morphology between catalysts that induced growth of CNTs and those that did not. Surface roughness was present on catalysts with same H₂ conditions, which results in dense vertical CNT growth (+5 minutes). In addition, examination of the samples introduced to H₂ at 600°C revealed the same surface roughness on the edges of the substrate where vertical and long CNTs were grown. However, in the center, where no carbon tubes were visible, showed a smooth morphology. This morphology was similar to the samples that were not exposed to heat or gases. From the difference in H₂ introduction between samples, we

conclude that H₂ affected the surface morphology. In addition, the differences observed on the edges and in the center of the samples could be a result of the flow pattern of gases, boundary layer thickness, or diffusion of gases over the catalyst and substrate. Therefore, an optimal flow rate of gases over the catalyst is extremely important in achieving carbon nanotube growth, as shown by most experimental protocols for CNT growth. The edges of the sample could have received a different amount of gas flow resulting in different morphologies.

5.3 Catalyst Chemical State

The catalyst chemical state inspected by XPS confirmed that the Fe exposed to ambient gases did not exist as pure Fe, but in oxidized form. The binding energy of pure Fe (Fe 2p_{3/2}) is 706.8eV, which was not seen in our XPS data. The oxidation of Fe in atmospheric conditions has also separately been verified by Park et al. [3]. The Fe, in our experiment, was present initially as a mixture of α -Fe₂O₃, FeO, and Fe₃O₄.

However, when these catalysts were exposed to H₂ at different time points and the high temperatures required for CNT growth, binding energy differences resulted indicating that the Fe catalyst chemical state had changed. With the samples, which were slowly cooled, increasing exposure to hydrogen showed higher binding energies for Fe compared to the reference and Ar only treated samples. The corresponding chemical states indicated that the H₂ was reducing the initially oxidized iron catalyst. In theory, H₂ exposure has been reported to facilitate surface mobility of metals atoms and clusters [10]. As a result, pretreatment with H₂ should have induced a high density of growth, but in our experiment the yield of CNTs was extremely low when introduced during the temperature ramp stage. A possible explanation is that the actual chemical state of the

catalyst hinders CNT growth when H₂ is introduced early as in the temperature ramp stage.

At time points where CNTs were present in low density (400°C and -15 minutes), there was a large in change binding energy between the two samples. We conclude that there may be multiple states of iron oxide, which catalyzes growth of CNTs; however, CNT growth is not optimal during chemical transitions between these oxidation states. Baker et al. reported that FeO, Fe₂O₃, and Fe all have catalytic activity, but FeO is the most active [18]. Hence, in our experiment, we confirm that these states catalyze CNT growth, but states in which they are transitioning between these different oxides may not.

Differences in binding energy were also observed in the samples, which were slowly cooled and rapidly cooled. The largest binding energy differences were observed in the samples, which had low yields of growth (400°C and -15 minutes). This change may have been observed because of the cooling conditions. However, if this were the case, then the samples introduced at 0 minutes (fast cooled and slow cooled) should have seen a similar change due to cooling effects, but the binding energies for Fe and alumina were exactly the same in both types of cooling. Hence, the change in binding energy between slow cooled and fast cooled must be associated with the additional 15 minutes of exposure to H₂ at 770°C.

5.4 Proposed Model

The model, which we propose, is based on the fact that even in highly pure gases such as Ar (99.9995%, <0.5 PPM of O₂) used in this system, enough oxygen is always present for oxidation of Fe. Therefore, exposure to hydrogen is essential in the rapid catalyzation of carbon nanotubes. When H₂ is present from the beginning, the Fe catalyst

particles, which are already slightly oxidized, cannot be oxidized further. As a result, it remains in a chemical state, which shows catalytic activity towards CNT growth.

However, when H₂ is introduced during temperature ramp, further oxidation of Fe has taken place because H₂ was not initially present to react with the O₂ molecules.

Therefore, the resulting chemical state of the catalyst and the long exposure to H₂, which reduces the oxidized iron, may curb CNT growth. In a study by Wen et al., an optimal amount of H₂ pretreatment was noted in which too much reduction decreased the yield of CNTs while the too little also decreased the subsequent yield of CNTs. This may be the phenomenon observed in our study.

When H₂ was introduced later in the growth process, the Fe catalysts were oxidized over a period of greater than 40 minutes at high temperatures and the oxidation state change of Fe was verified by XPS. The introduction of H₂ had an effect of reducing these particles and as a consequence a rough surface morphology emerged, which was clearly correlated to a high yield of CNT growth.

Surface morphology was shown as a possible factor in CNT growth. de los Arcos et al. reported that differences in contact angles of Fe result in different contact areas with the substrate [5]. Furthermore, Fe in different oxygen partial pressures gives different contact angles on single crystalline alumina. So in a diffusion-based model proposed by Kanzow, “the contact area of the particle with the substrate provides a cooler region where precipitation of the carbon can take place. A reduced contact surface would therefore result in a slower growth rate” [19]. As a result, the surface roughness where CNTs were grown provides evidence that wettability of Fe particles may play an important role.

Chapter 6

Conclusion

Our results clearly demonstrate that there is a correlation between H₂ exposure, the catalyst oxidation state and morphology, and growth of CNTs. H₂ was observed to suppress the growth of CNTs when introduced during the temperature ramp, but was essential for the growth of long carbon nanotubes when introduced during later points of annealing and during the growth stage. In addition, H₂ was observed to initiate fast growth of CNTs, as verified by SEM images of CNTs grown with only 1 minute and 30 seconds of H₂.

For different time points of H₂ introduction, we studied the catalyst chemical state and morphology, and correlated them with the mode of growth of CNTs. These studies revealed that even though 1 nm of pure Fe was deposited on the alumina / Si substrate, the catalyst was oxidized due to atmospheric presence of O₂. In addition, H₂ was seen to reduce the Fe catalyst, but to different chemical states, not including pure Fe. Different oxidized states of Fe were shown to yield CNTs, but certain states, such as the FeOOH state, yielded very few CNTs while more stable states resulted in a high yield of CNTs. AFM inspection of the catalyst morphology also showed that there is a connection between surface roughness and CNT growth.

Therefore, we were able to propose a model in which oxidation of Fe and the reduction of the oxidized catalyst by H₂ plays an important role in the initiation of carbon nanotube growth. The interaction of the catalyst and H₂ controls the chemistry and morphology of the catalyst particles and as a result the yield of CNTs and their characteristics.

Chapter 7

Future Research

For future research we would like to further examine the role of oxygen in CNT growth. To further probe oxygen's role, it would be optimal to develop a system in which no oxygen is unintentionally present during the growth of CNTs. In addition, it would be interesting to explore the effects of H₂ and O₂ on other catalysts, such as Ni, and Co, or on other substrate, for CNT growth. This would shed light on the role of oxygen and hydrogen with respect to oxidation and reduction and the chemical state of the metal catalyst, which induces CNT growth. Another area of interest is the determining of type of CNTs grown with various time points of hydrogen introduction. Raman Spectroscopy can be utilized to examine the CNTs to determine their structure and purity. We would also like to examine the catalyst particles *in-situ* to observe the chemical states during the actual growth of CNTs. Others areas of research to further clarify the mechanism of CNT growth would be examination of particle crystalline state, orientation with respect to the substrate, and the contact angle.

Bibliography

- [1] Baker R T K, Alonzo J, Duesic J, Yates D 1982 *J. Catal.* **77** 74-84.
- [2] Wen H C, Yang K, Ou K, Wu K, Luo R 2005 *Microelectronic Engineering* **82** 221-227.
- [3] Park J B, Choi G S, Cho Y S, Hong S Y, Kim D 2002 *Journal of Crystal Growth.* **244** 211 - 217.
- [4] Lee C J, Kim D W, Lee T J, Choi Y C 1999 *Chem Phys. Let.* **213** 461-468
- [5] de los Arcos T, Garnier M, Seo J W, Oelhafen P 2004 *J. Phys. Chem. B* **108** 7727-7734.
- [6] Homma Y, Yamashita T, Finnie P, Tomita M 2002 *Jpn. J. Appl. Phys.* **41** 89-91.
- [7] Choi Y C, Kim D W, Lee T J, Lee C J 2001 *Synthetic Metals* **117** 81-86.
- [8] Xiong G Y, Suda Y, Wang D Z, Huang J Y 2005 *Nanotechnology* **16** 532-535.
- [9] Zhang G, Mann D, Zhang L, Javey A 2005 *PNAS* **102** **45** 16141-16145.
- [10] Cantor M, Hofmann S, Pisana S, Scardaci V, Parvez P, Robertson J 2006 *Nano Letters*
- [11] Chhowalla M, Teo K, Ducati C, Rupesinghe 2001 *J. Appl. Phys.* **90** 10.
- [12] Hash D B, Meyyappan M 2003 *J. Appl. Phys.* **93** 1.
- [13] Sinnott S B, Andrews R, Qian D, Rao A M *Chem. Phys. Let.* **315** 25-30.
- [14] Lee C J, Park J H 2001 *Carbon* **39** 1891-1896.
- [15] Dresselhaus M S, Dresselhaus G 1998 *Physics World* February
- [16] Iijima S. 1991 *Nature* **354** 56-8.
- [17] Meyyyappan M. *Carbon Nanotubes: Science and Applications* CRC Press New York 2004.

- [18] Baker R T K 1989 *Carbon* **27** 315-323.
- [19] Kanzow H, Ding A 1999 *Phys. Rev. B.* **60** 11180-11186.
- [20] Thompson C V, *Proc. of the Symposium on Future Integrated Systems*, University of Cambridge, August 2005, published by MTP, p.52 (2005).